

A dynamical model for wavefunction collapse via non-Hermitian Hamiltonian

Gurpahul Singh,^{*} Ritesh Kumar Singh,[†] and Soumitro Banerjee[‡]

Department of Physical Sciences, Indian Institute of Science Education and Research Kolkata, Mohanpur, 741 246, India

(Dated: March 23, 2023)

Ever since the formulation of quantum mechanics, there is very little understanding of the process of the collapse of a wavefunction. We have proposed a dynamical model to emulate the measurement postulates of quantum mechanics. We postulate that a non-Hermitian Hamiltonian operates during the process of measurement, which evolves any state to an attracting equilibrium state, thus, mimicking a “collapse”. We demonstrate this using a 2-level system and then extend it to an N-level system. For a 2-level system, we also demonstrate that the dynamics generated by the Lindblad master equation can be replicated as an incoherent sum of the evolution by two separate non-Hermitian Hamiltonians.

I. INTRODUCTION

Any standard quantum mechanics course or textbook [1, 2] begins with a set of postulates. Three of them are termed the “measurement postulates”, which we are currently interested in. These are:

- P1. A wavefunction, upon measurement of an observable, will always “collapse” to one of the eigenstates of the operator corresponding to that observable.
- P2. The probability of collapse to a particular eigenstate depends on the probability amplitudes associated with each eigenstate in the linear decomposition of the wavefunction.
- P3. Any repeated measurement immediately after a collapse gives the same eigenstate.

In case of an energy measurement, a closed quantum system continues to be in the collapsed energy eigenstate.

The measurement postulates in QM have been around for almost a century. Throughout this time, physicists and philosophers have tried to come up with some kind of explanation or motivation for these postulates. Bohr-Einstein debates [3] were one of the earliest examples of discussions on the framework of QM in general. Later, the well-known EPR paper [4] led to the understanding of the phenomenon of entanglement. Eventually, the Copenhagen interpretation [5] prevailed, which states that a quantum state is intrinsically indeterminate until a measurement is made, and the act of measurement creates the state that is observed.

This particular aspect of the measurement problem—the collapse of the wavefunction—has been an area of active research. Numerous models have been proposed to explain its nature. One of the earliest models was the “hidden variable theory” that stemmed from the EPR paper. A non-local hidden variable theory

was the De-Broglie Bohm theory [6]. Other models that followed were Everett many-worlds interpretation [7], von Neumann-Wigner interpretation [8], Ghirardi-Rimini-Weber (GRW) theory [9], Continuous Spontaneous Localization (CSL) model [10, 11], Diosi-Penrose (DP) model [12, 13], Relational QM [14] and decoherence model of collapse [15].

In 1964, John Bell came up with his famous theorem [16], which showed that local hidden variable theories and quantum mechanics would yield different predictions regarding the outcome of an experiment. Subsequent experiments [17, 18] vindicated the predictions of QM, although there is still minor skepticism about experimental setups or the theorem itself [19]. Leggett-Garg inequality [20] and CHSH inequality [21] have also been used in experiments to further confirm the claim made by Bell.

Since the measurement is a physical process, we treat it as occurring over a finite interval. During this interval, the apparatus interacts with the system, and the whole dynamics is governed by a Hamiltonian acting on the combined Hilbert space of the system and apparatus. This leads to *leaking* of probabilities from the system to the apparatus and vice-versa. When seen from the point of view of the system Hilbert space alone, the dynamics appears to be governed by a non-Hermitian Hamiltonian.

Non-Hermitian Hamiltonians with \mathcal{PT} -symmetry (where \mathcal{P} is the reflection operator in space and \mathcal{T} is the time-reversal operator) have been of interest ever since their introduction in the late 1990s. Starting from Bender [22, 23], a general framework of QM has been formulated by replacing the condition of Hermiticity with a generic anti-linear symmetry [24]. There has been growing interest in the experiments associated with these non-Hermitian Hamiltonians [25, 26]. The earliest experimental observations were made in optics [27–29]. Experiments were also conducted in other physical systems such as mechanics [30], electronics [31–33], microwaves [34], nonlinear systems [35] and very recently in open quantum systems [36, 37] and quantum many-body systems [38].

If a non-Hermitian Hamiltonian has an antilinear symmetry (such as \mathcal{PT} -symmetry), then its eigenvalues are real or appear as complex conjugate pairs [39]. For our model, we will be working with non-Hermitian Hamilto-

^{*} Electronic address : gs18ms106@iiserkol.ac.in

[†] Electronic address : ritesh.singh@iiserkol.ac.in

[‡] Electronic address : soumitro@iiserkol.ac.in

nians without any requirement of an anti-linear symmetry. Using such a non-Hermitian Hamiltonian H_m , one can obtain a new von Neumann equation which is nonlinear in nature [40]. If H_m has complex eigenvalues, then a state ρ under time evolution would reduce to the eigenvector of H_m having the largest imaginary part of the eigenvalue. In other words, the eigenvector with the largest imaginary part of the eigenvalue will become the attractor of the dynamics. We have used this feature to propose a dynamical model for a state to converge to an eigenvector, i.e., the wavefunction collapse.

The organization of the paper is as follows: in Sec. II, we introduce the nonlinear von Neumann equation that dictates the time evolution of a state when a non-Hermitian Hamiltonian is applied and study its implications. In Sec. III, we demonstrate the collapse using our model for a two-level system state. Then we extend the same formalism to N-dimensional Hilbert space and consider 4-level state to study the effect of degeneracy in real and imaginary part of the eigenvalues. Three different diagonal non-Hermitian Hamiltonians have been separately discussed in Sec. IV. One of the cases turns out to have a connection to the Markovian dynamics of the Lindblad master equation. In Sec. V, we discuss the challenges related to our model and summarize the results of our work.

II. THE NONLINEAR VON NEUMANN EQUATION

Let us consider a non-Hermitian Hamiltonian H of the form $H = H_h - iH_a$ where H_h and H_a are the Hermitian and anti-Hermitian parts. Both H_h and H_a are Hermitian: $H_h^\dagger = H_h$ and $H_a^\dagger = H_a$. The density matrix ρ of a system, evolved via the Hamiltonian H will follow [40]

$$\dot{\rho} = -i[H_h, \rho] - \{H_a, \rho\} + 2 \text{tr}(\rho H_a)\rho \quad (1)$$

which is similar to the nonlinear Schrödinger equation mentioned in [41]. The nonlinearity comes in because of the last term on the RHS introduced to preserve the trace of ρ . The evolved state $\rho(t)$ is then given by

$$\rho(t) = \frac{e^{-iHt}\rho(0)e^{iH^\dagger t}}{\text{Tr}(e^{-iHt}\rho(0)e^{iH^\dagger t})} \quad (2)$$

where we see a time dependent normalisation factor.

For most of our analysis, we will investigate how the state evolves on the Bloch sphere. We can write a general density matrix as

$$\rho = \frac{1}{2}(\mathbb{I} + x\sigma_x + y\sigma_y + z\sigma_z)$$

where σ_i are the Pauli matrices and x, y, z represent the coordinates of the state on (or inside) the Bloch sphere. Each coordinate $i = \text{Tr}(\rho\sigma_i)$ and $x^2 + y^2 + z^2 \leq 1$.

Let $H = \sigma_x - i\gamma\sigma_z$ such that $H_h = \sigma_x$ and $H_a = \gamma\sigma_z$, where $\gamma \geq 0$. We put the expression for ρ, H_h and H_a in

equation (1), multiply with the Pauli matrices and take the trace to obtain:

$$\dot{x} = \text{Tr}(\dot{\rho}\sigma_x) = 2\gamma xz \quad (3a)$$

$$\dot{y} = \text{Tr}(\dot{\rho}\sigma_y) = 2\gamma yz - 2z \quad (3b)$$

$$\dot{z} = \text{Tr}(\dot{\rho}\sigma_z) = 2\gamma z^2 + 2y - 2\gamma \quad (3c)$$

The fixed points of the dynamics mainly present two cases:

$$\dot{x} = 0 \Rightarrow xz = 0.$$

So, either $x = 0$ or $z = 0$. For $z = 0$, $\dot{y} = 0$. $\dot{z} = 0 \Rightarrow y^* = \gamma$. So, we have a line of fixed points at $y = \gamma$ (parallel to x -axis) in the x - y plane. The fixed points on the surface of Bloch sphere have the constraint that $(x^*)^2 + (y^*)^2 = 1$. And so $(x^*)^2 = \pm\sqrt{1-\gamma^2}$. Thus, on the Bloch sphere, we have the fixed points $(x, y) = (\pm\sqrt{1-\gamma^2}, \gamma)$. Also, note that for x to be real, γ must be less than 1.

So, the $z = 0$ case of fixed points is valid for $\gamma \leq 1$ which is also the parameter region where H is \mathcal{PT} -symmetric [22, 40] or it has real eigenvalues. Analysing the stability of the line of fixed points for $z = 0$ case, we find that all these points are centers. So, locally, the trajectories around the fixed points are circles. In fact, from (3), at $\gamma = 0$, we can see that we have exactly circular orbits for any initial condition in the y - z plane (for both pure and mixed states).

The case we would be interested in is of $x = 0$. The fixed points come out as

$$\begin{aligned} \dot{y} = 0 &\Rightarrow y^* = \frac{1}{\gamma} \\ \dot{z} = 0 &\Rightarrow z^* = \pm \frac{\sqrt{\gamma^2 - 1}}{\gamma} \end{aligned}$$

And we see that $y^{*2} + z^{*2} = 1$, which means that the only fixed points in this case are on the Bloch sphere, in the y - z plane. Since z^* has to be real, these fixed points start existing after $\gamma \geq 1$. The stability of these fixed points show that the point $(0, \frac{1}{\gamma}, \frac{\sqrt{\gamma^2-1}}{\gamma})$ has all positive eigenvalues, while the point $(0, \frac{1}{\gamma}, -\frac{\sqrt{\gamma^2-1}}{\gamma})$ has all negative real eigenvalues indicating a source and a sink respectively.

Let $\epsilon = \sqrt{\gamma^2 - 1}$. Then the eigenvalues of H for $\gamma > 1$ are $+i\epsilon$ and $-i\epsilon$ with the corresponding eigenvectors as

$$|R_1\rangle = \frac{1}{\sqrt{2\gamma(\gamma + \epsilon)}} \begin{pmatrix} 1 \\ i(\gamma + \epsilon) \end{pmatrix} \quad (4a)$$

$$|R_2\rangle = \frac{1}{\sqrt{2\gamma(\gamma - \epsilon)}} \begin{pmatrix} 1 \\ i(\gamma - \epsilon) \end{pmatrix} \quad (4b)$$

respectively. If we find the coordinates for these eigenvectors on the Bloch sphere, they happen to coincide exactly with the two fixed points: $|R_2\rangle$ eigenvector being the sink and $|R_1\rangle$ being the source.

In summary, we have two disjoint parameter regions (except $\gamma = 1$ where the transition takes place). For $\gamma < 1$ or \mathcal{PT} -symmetric region, we have a line of fixed points with closed periodic trajectories. $\gamma > 1$ is called the \mathcal{PT} broken region since H has complex eigenvalues [22]. Here we see a sink and a source existing on the Bloch sphere. This also means that any initially mixed state would finally end up at the surface of the Bloch sphere (purification). This case is important for our measurement postulates as we will see in the next section.

III. THE MEASUREMENT HAMILTONIAN

To model the collapse process or emulate the measurement postulates, we lay down the following assumptions:

- A1. There is a finite time during which the measurement takes place. We take t_i as the point where this process starts and t_f when it ends.
- A2. In between t_i and t_f , a “measurement Hamiltonian” H_m acts on the state. H_m is a non-Hermitian Hamiltonian with complex eigenvalues.

Before the measurement starts, the state is either a static state (a point on the Bloch sphere) or one that is oscillating on the Bloch sphere due to some Hermitian driving Hamiltonian. Also, any \mathcal{PT} -symmetric Hamiltonian with real eigenvalues can be made Hermitian using some similarity transformation [42]. Thus, in general, we can have a \mathcal{PT} -symmetric Hamiltonian H with real eigenvalues driving the state before the measurement and then a \mathcal{PT} -broken Hamiltonian H_m operates during the measurement from t_i to t_f . In that time period, the state would go to one of the eigenvectors of H_m which can be seen from our analysis in section II.

After t_f , we have H acting again, but because of the measurement process, the state should remain at the eigenvector of H_m (the collapse). For this to happen, the eigenvector to which H_m sends the state must exactly match with the eigenvector of H . Let us demonstrate this using a two-level state.

A. Two-level state

For our further discussion, we consider a specific Hamiltonian $H = \sigma_x - i\gamma\sigma_z$ since it has been discussed widely in many earlier papers on \mathcal{PT} -symmetric non-Hermitian QM [40, 43]. This is the driving Hamiltonian that operates on the state before t_i and after t_f . The eigenvalues of H are real for $|\gamma| < 1$ [40]. Fig. 1 shows how the Bloch sphere trajectories would look like for different initial states for $\gamma = 0$ (Hermitian case).

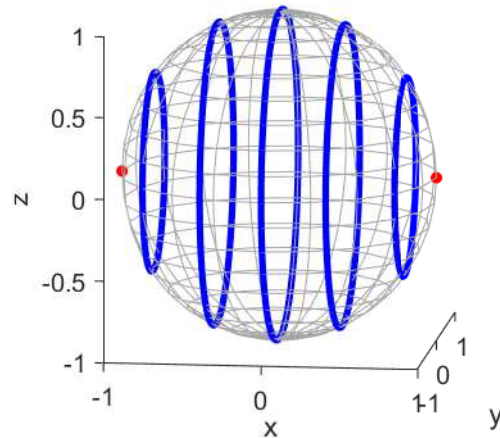


FIG. 1. Bloch sphere trajectories (blue) of different initial states evolved via $H = \sigma_x$. The evolved states are obtained using equation (2). The states (all pure) oscillate on the surface of the Bloch sphere in the x - y plane and the picture is exactly the same for all values of $\gamma < 1$. Red dots indicate the eigenvectors of H .

The eigenvalues of H are $+E$ and $-E$, where $E = \sqrt{1 - \gamma^2}$. Its corresponding eigenvectors are

$$|R_+\rangle = \frac{1}{\sqrt{2}} \begin{pmatrix} 1 \\ i\gamma + E \end{pmatrix} \quad (5a)$$

$$|R_-\rangle = \frac{1}{\sqrt{2}} \begin{pmatrix} 1 \\ i\gamma - E \end{pmatrix} \quad (5b)$$

Now, for an energy measurement, the H_m should be able to send an initial state to either $|R_+\rangle$ or $|R_-\rangle$. Say, we take $H_m = \sigma_x - i\gamma_m\sigma_z$ where $|\gamma_m| > 1$ for H_m to have complex eigenvalues (see A2). Let $\epsilon = \sqrt{\gamma_m^2 - 1}$. So, H_m makes a state converge to the eigenstate corresponding to $+i\epsilon$ eigenvalue (the attractor state) which is

$$|R_{m+}\rangle = \frac{1}{\sqrt{2\gamma_m(\gamma_m + \epsilon)}} \begin{pmatrix} 1 \\ i(\gamma_m + \epsilon) \end{pmatrix} \quad (6)$$

as can be seen from (4a). In order for the state to remain collapsed after t_f , we need to match $|R_{m+}\rangle$ with whichever of the two eigenvectors of H our state collapses to. If the state collapses to $+E$, we match $|R_{m+}\rangle$ with $|R_+\rangle$; if it collapses to $-E$, we match it with $|R_-\rangle$. Thus, this is, as yet, a *deterministic* model for the collapse of the wavefunction. We come back to this in section VI.

The strategy we follow to match the eigenstates is the following. First we diagonalise H_m by writing it in its eigenvector basis:

$$H_m^D = \begin{bmatrix} i\epsilon & 0 \\ 0 & -i\epsilon \end{bmatrix}$$

The attractor state in this basis becomes $|R_{m+}^D\rangle = \begin{pmatrix} 1 \\ 0 \end{pmatrix}$. Then we will try to find a similarity transformation for

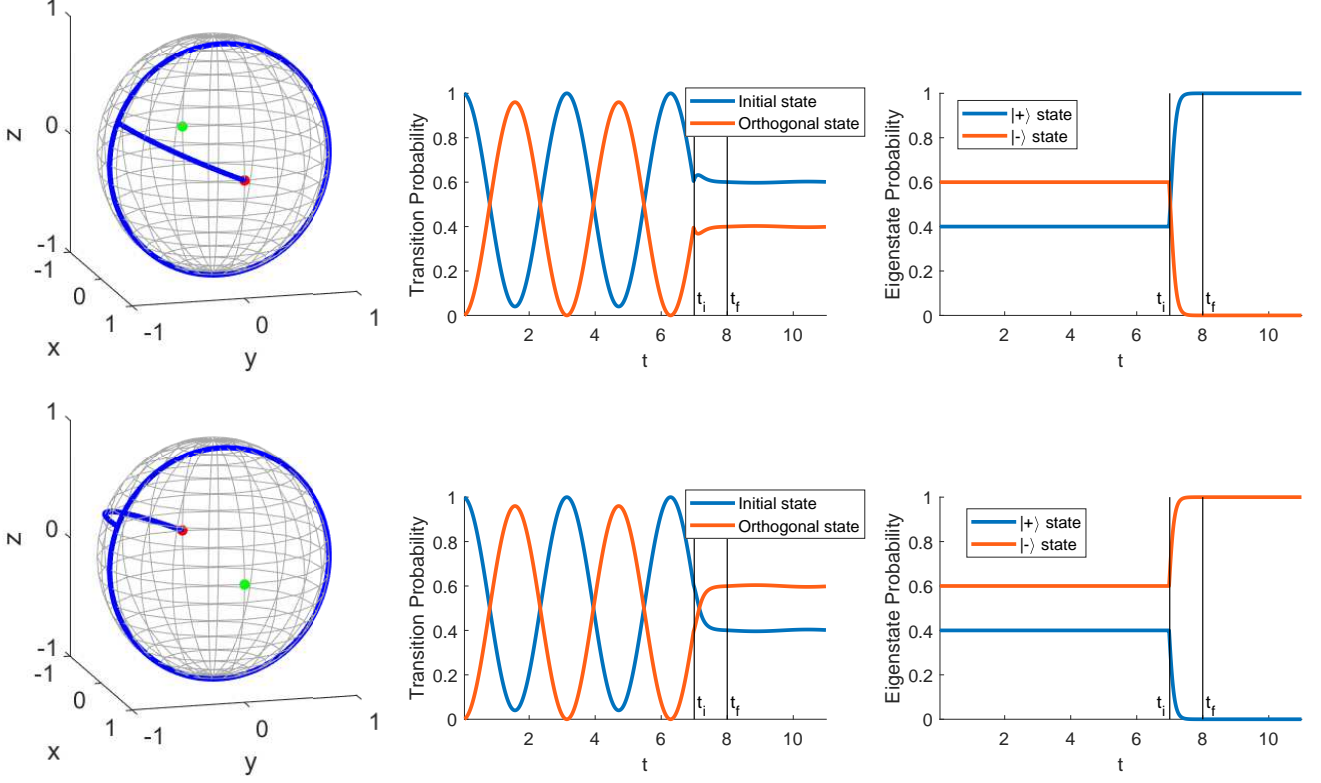


FIG. 2. (two graphs on the left) Bloch sphere trajectory of a state evolved using (2) with $H = \sigma_x$ before $t_i = 7$ and after $t_f = 8$ and with $H_m = i\epsilon\sigma_x$ (top left) and $H_m = -i\epsilon\sigma_x$ (bottom left) in between t_i and t_f . $\epsilon = \sqrt{\gamma_m^2 - 1}$ and $\gamma_m = 3$. The red and green markers denote the sink and the source respectively. (middle) Probability of being in the initial state (blue) and its orthogonal state (orange). We can see that the state oscillates before t_i and the oscillations die down when H_m acts. (top right) The probability of being in the $|+\rangle$ state grows to 1, while being in $|-\rangle$ goes to 0 while the opposite happens for the bottom right graph.

H_m such that after the transformation, it should be the attractor state that matches with the eigenvector of H where collapse happens.

Let the transformed matrix be

$$H'_m = SH_m^D S^{-1} \quad (7)$$

For attractor eigenstate $|R_{m+}^D\rangle$ of H_m^D ,

$$\begin{aligned} H_m^D |R_{m+}^D\rangle &= i\epsilon |R_{m+}^D\rangle \\ \Rightarrow H'_m (S |R_{m+}^D\rangle) &= i\epsilon (S |R_{m+}^D\rangle), \end{aligned}$$

which means that the eigenvector of H'_m corresponding to the same eigenvalue of H_m^D will be $S |R_{m+}^D\rangle$.

Let us say that the state of H to which the initial state collapses is $|R_+\rangle$. So, we will equate $|R_+\rangle$ with $S |R_{m+}^D\rangle$.

$$\frac{1}{\sqrt{2}} \begin{pmatrix} 1 \\ i\gamma + E \end{pmatrix} = S \begin{pmatrix} 1 \\ 0 \end{pmatrix} \quad (8)$$

Assuming $\det(S) = 1$, the expressions of S and S^{-1}

become

$$S = \begin{bmatrix} \frac{1}{\sqrt{2}} & b \\ \frac{i\gamma + E}{\sqrt{2}V} & \sqrt{2} + \frac{b(i\gamma + E)}{V} \end{bmatrix}$$

and

$$S^{-1} = \begin{bmatrix} \sqrt{2} + \frac{b(i\gamma + E)}{V} & -b \\ \frac{-(i\gamma + E)}{\sqrt{2}V} & \frac{1}{\sqrt{2}} \end{bmatrix}.$$

where b is a free parameter. Choosing $b = \frac{i\gamma - E}{\sqrt{2}}$ and renaming H'_m to H'_{m+} (indicating collapse to $|R_+\rangle$), we obtain

$$H'_{m+} = i\epsilon \begin{bmatrix} 0 & E - i\gamma \\ E + i\gamma & 0 \end{bmatrix}. \quad (9)$$

If we take $\gamma = 0$, which means we have $H = \sigma_x$ in the beginning (oscillations in the y-z plane), then H'_{m+} takes the form

$$H'_{m+} = i\epsilon \begin{bmatrix} 0 & 1 \\ 1 & 0 \end{bmatrix} = i\epsilon\sigma_x. \quad (10)$$

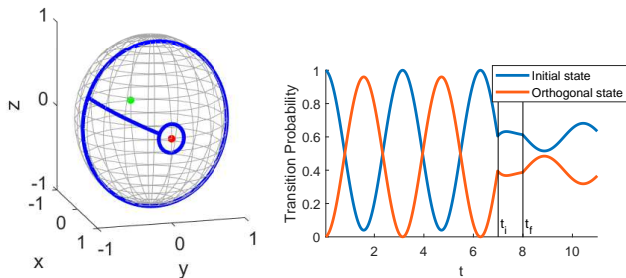


FIG. 3. Here $H_m = i\epsilon\sigma_x$, $\gamma_m = 1.5$, $t_i = 7$ and $t_f = 8$. We see that for reduced value of γ , convergence to the fixed point does not happen, instead the state starts oscillating around the fixed point. This shows that for higher value of γ , we have higher rates of convergence and vice-versa.

We see that the eigenvectors of H and H'_{m+} are the same but the former is Hermitian while H'_{m+} is non-Hermitian. So, once H'_{m+} evolves an initially oscillating state to one of the fixed points, it would stay there even after t_f . This is shown in the top-left panel in Fig. 2. All the plots are generated by taking an initial state and evolving it using (2). In the top-middle panel of Fig. 2, we show the probability of being in the initial state, i.e., $\text{Tr}(\rho(t)\rho(0))$ in blue and the probability of being in the orthogonal state, $\text{Tr}(\rho(t)(\mathbb{I}-\rho(0)))$, in orange. The probabilities of being in the $|+\rangle$ (blue) and in $|-\rangle$ state (orange) are shown in the top-right panel.

If the state were to collapse to eigenstate $-E$, the only change to the measurement Hamiltonian would be to replace E by $-E$ in (9) $\Rightarrow H'_{m-} = -i\epsilon\sigma_x$ for $\gamma = 0$. The graphs are shown in the bottom row in Fig. 2.

In both the cases above, the degree of collapse to a chosen state can be parameterized as

$$\kappa = 1 - e^{-\gamma_m(t_f - t_i)}$$

which tends to 1 for large enough values of $\gamma_m(t_f - t_i)$.

The speed of convergence is higher for higher γ_m and vice-versa. That means if the system-apparatus coupling is smaller, the state would collapse slower as shown in Fig. 3 where we have reduced γ_m by a factor of 2. Here we see that the state has not converged (collapsed) to the fixed point, but rather oscillates around it. Similarly, doubling the measurement interval here restores the degree of collapse as shown in Fig. 4.

B. Extension to N-level system

From our analysis in the last subsection, we see that both H and $H'_{m\pm}$ commute with each other. We can, in fact, generalize the concept by writing everything in the basis of the Hermitian Hamiltonian H . If we diagonalize H , then H_m is also diagonal with its eigenvalues replaced by complex numbers. Thus, we would not have to do a similarity transformation or matching of the

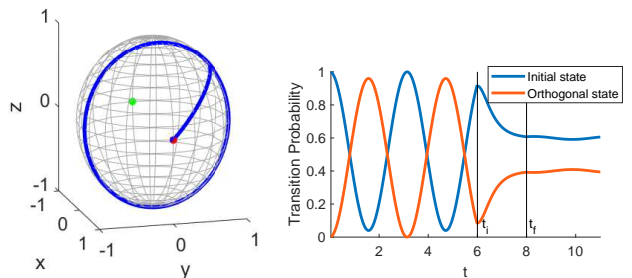


FIG. 4. Here $H_m = i\epsilon\sigma_x$, $\gamma_m = 1.5$, $t_i = 6$ and $t_f = 8$. Doubling the measurement time interval allows the state to get closer to the fixed point. This means that given enough time, any state would approach the fixed point asymptotically.

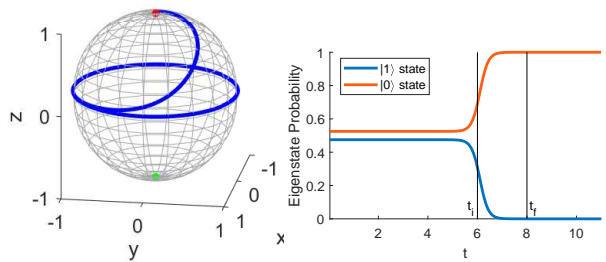


FIG. 5. (left) Bloch sphere trajectory of a two-level state evolved using $H_m(t)$ (13). The state converges to the North pole as is also evident from the eigenstate probability (right). $\gamma = 3$, $t_i = 6$ and $t_f = 8$.

eigenstates. It is also observed that an initial state converges to the eigenvector which has an eigenvalue with the largest imaginary part. One way to construct H_m in the diagonal case is to add an imaginary number having a positive part to one of the eigenvalues which would lead to the collapse to the corresponding eigenvector. The Hermitian Hamiltonian H in the eigenvector basis can be written as

$$H = \sum_i \lambda_i |\phi_i\rangle\langle\phi_i|, \quad (11)$$

then $H_{m,j}$ required to collapse to $|\phi_j\rangle$ is given as

$$H_{m,j} = i\gamma_m |\phi_j\rangle\langle\phi_j| + \sum_i \lambda_i |\phi_i\rangle\langle\phi_i| \quad (12)$$

where $\gamma_m > 0$. Combining equation (11) and (12) into one single time dependent Hamiltonian $H_j(t)$, we get

$$H_j(t) = \sum_i \lambda_i |\phi_i\rangle\langle\phi_i| + i\gamma f(t) P_j \quad (13)$$

where $P_j = |\phi_j\rangle\langle\phi_j|$ is the projection operator to $|\phi_j\rangle$, and $f(t)$ is a switching function which switches on the second term at $t = t_i$ and switches it off at $t = t_f$. In the following simulations, we use $f(t)$

$$f(t) = [\tanh(\gamma(t - t_i)) - \tanh(\gamma(t - t_f))]/2.$$

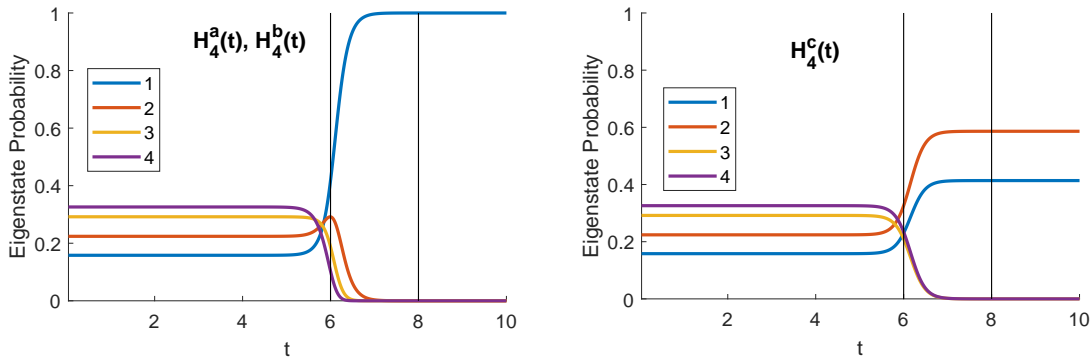


FIG. 6. (left) Probability of being in one of the eigenstates for a 4-level state when either (a) both real and imaginary parts of the eigenvalues are non-degenerate ($H_4^a(t)$) or (b) there is degeneracy only in the real part of the eigenvalues ($H_4^b(t)$). (right) (c) There is degeneracy in the largest imaginary part of the eigenvalues while the real part of the eigenvalues is non-degenerate. $\gamma = 3$, $t_i = 6$ and $t_f = 8$.

We note that γ_m (12), i.e., imaginary part of eigenvalue decides the speed of collapse while γ appearing in the switching function above controls the speed of switching. To reduce the number of free parameters, we choose $\gamma = \gamma_m$ in our simulations. This has been already taken into account in equation (13).

We use this Hamiltonian $H_m(t)$ to simulate 2-level dynamics. The Bloch sphere trajectory and eigenstate probability graph are shown in Fig. 5. Initially, the state oscillates along the equator and then spirals toward the North pole in the measurement duration. The diagonal of the Hamiltonian makes the oscillate in the xy plane initially and the smooth transition is caused by the smoothness of $f(t)$.

We have seen that adding a positive imaginary part would make the state collapse to the corresponding eigenvector ($|\phi_j\rangle$ in (13)). Let us now see the effect of degeneracy in the real and imaginary parts of the eigenvalues on the collapse using three cases of $N = 4$ Hamiltonians. For dimensions $N > 2$, Bloch-sphere-like representations are not possible, so we show only the eigenstate probabilities to demonstrate collapse.

Case a. Both the real part and the imaginary part of the eigenvalues are non-degenerate. We choose the Hamiltonian to be

$$H_4^a(t) = \text{dia}(1, 2, 3, 4) + i\gamma f(t)\text{dia}(4, 3, 2, 1)$$

where $\gamma = 3$. Hence, the collapse should happen to the eigenstate with eigenvalue 1 because it has the largest imaginary part. This is precisely what is seen in the left panel of Fig. 6. All other eigenstates, although also having positive imaginary parts, would start decaying to 0 because of the relative difference in the imaginary parts.

Case b. The imaginary parts are non-degenerate while the real parts are degenerate.

$$H_4^b(t) = \text{dia}(1, 1, 1, 4) + i\gamma f(t)\text{dia}(4, 3, 2, 1)$$

Here, the collapse again happens to the 1st eigenstate, further confirming that convergence is only determined

by the largest imaginary part. The graph is exactly the same as the left panel in Fig. 6.

Case c. The real parts are non-degenerate while the imaginary parts are degenerate

$$H_4^c(t) = \text{dia}(1, 2, 3, 4) + i\gamma f(t)\text{dia}(0, 0, -1, -1)$$

In this case, we have non-positive imaginary parts. The largest imaginary parts being degenerate (having value = 0) means that there is no preferred eigenstate to collapse to. The initial state reduces to a two-dimensional subspace spanned by the first two eigenstates, while the probability of being in the other two eigenvectors decays to 0 as can be seen in the right panel of Fig. 6. We also see that the probabilities for the first two eigenstates get rescaled to preserve the total probability but the ratio of the probability coefficients remains the same. So, in our model, the collapse would take place only if there is an eigenvalue with a unique largest imaginary part.

Thus, we have shown that by diagonalizing the complex non-Hermitian measurement Hamiltonian, we have been able to easily extend the collapse protocol to higher dimensional Hilbert space. We have also shown that the collapse to a particular eigenstate depends only on the imaginary part of the eigenvalues and requires the largest imaginary part to be unique.

IV. CONNECTION TO THE LINDBLAD FORMALISM

Let us now see how a time evolved density matrix $\rho(t)$ looks like when evolved using a general non-Hermitian Hamiltonian H . For this we use

$$\rho(0) = \frac{1}{2}(\mathbb{I} + r_x\sigma_x + r_y\sigma_y + r_z\sigma_z) = \frac{1}{2}(\mathbb{I} + \vec{r} \cdot \vec{\sigma})$$

where r_x, r_y, r_z are all real. We choose a Hamiltonian

$$H = R_0\mathbb{I} + R_1\sigma_x + R_2\sigma_y + R_3\sigma_z = R_0\mathbb{I} + \vec{R} \cdot \vec{\sigma}$$

where R_0, R_1, R_2, R_3 can be complex. Also,

$$H^\dagger = R_0^* \mathbb{I} + \vec{R}^* \cdot \vec{\sigma}.$$

Substituting H , H^\dagger and $\rho(0)$ in (2), we have $\rho(t) = \frac{N(t)}{\text{Tr}(N(t))}$ where $N(t)$ is

$$\begin{aligned} N(t) = & \frac{1}{2} e^{-i(R_0 - R_0^*)t} \{ \cos(pt) \cos(qt) (\mathbb{I} + \vec{r} \cdot \vec{\sigma}) \\ & + \frac{i}{q} \cos(pt) \sin(qt) (\mathbb{I} + \vec{r} \cdot \vec{\sigma}) (\vec{R}^* \cdot \vec{\sigma}) \\ & - \frac{i}{p} \cos(qt) \sin(pt) (\vec{R} \cdot \vec{\sigma}) (\mathbb{I} + \vec{r} \cdot \vec{\sigma}) \\ & + \frac{1}{pq} \sin(pt) \sin(qt) (\vec{R} \cdot \vec{\sigma}) (\mathbb{I} + \vec{r} \cdot \vec{\sigma}) (\vec{R}^* \cdot \vec{\sigma}) \} \end{aligned} \quad (14)$$

where $p = \sqrt{\vec{R} \cdot \vec{R}}$ and $q = \sqrt{\vec{R}^* \cdot \vec{R}^*}$. Let us take the initial state to be

$$|\psi(0)\rangle = c_1|0\rangle + c_2|1\rangle \Rightarrow \rho(0) = \begin{bmatrix} |c_1|^2 & c_1 c_2^* \\ c_1^* c_2 & |c_2|^2 \end{bmatrix}$$

so that we have $r_x = c_1 c_2^* + c_1^* c_2$, $r_y = i(c_1 c_2^* - c_1^* c_2)$, $r_z = |c_1|^2 - |c_2|^2$. And we consider a diagonal H with $R_1 = R_2 = 0 \Rightarrow p = R_3$, $q = R_3^*$.

Our results in the previous sections have shown that, broadly, there can be three ways we can send an initial state ρ to one of the eigenvectors of a Hamiltonian H_m .

Case A. We add an imaginary number $i\gamma$ where $\gamma > 0$ to one eigenvalue and subtract it from the other. This is like ‘‘pushing’’ the state towards one eigenvector (by adding $i\gamma$) and at the same time ‘‘pulling’’ it away from the other (by subtracting $i\gamma$). So, H_m would look like

$$\begin{aligned} H_m^A = & \begin{bmatrix} \lambda_1 + i\gamma & 0 \\ 0 & \lambda_2 - i\gamma \end{bmatrix} \\ & = \lambda_0 \mathbb{I} + (\omega + i\gamma) \sigma_z, \end{aligned} \quad (15)$$

where $\lambda_0 = \frac{\lambda_1 + \lambda_2}{2}$ and $\omega = \frac{\lambda_1 - \lambda_2}{2}$. So, $R_0 = \lambda_0$ and $R_3 = \omega + i\gamma$. We expand (14) and divide it by the trace to get the full expression of $\rho^A(t)$ as

$$\rho^A(t) = \begin{bmatrix} \frac{|c_1|^2}{|c_1|^2 + |c_2|^2 e^{-4\gamma t}} & \frac{c_1 c_2^* e^{-i2\omega t}}{|c_1|^2 e^{2\gamma t} + |c_2|^2 e^{-2\gamma t}} \\ \frac{c_1^* c_2 e^{i2\omega t}}{|c_1|^2 e^{2\gamma t} + |c_2|^2 e^{-2\gamma t}} & \frac{|c_2|^2}{|c_1|^2 e^{4\gamma t} + |c_2|^2} \end{bmatrix} \quad (16)$$

It is clear from the above equation that as $t \rightarrow \infty$, the off-diagonal terms go 0 (decoherence). The $\rho_{22}^A(t)$ element also goes to 0 while the $\rho_{11}^A(t)$ term goes to 1. Hence the state ultimately approaches $|0\rangle$ state given enough time. Also, the rate of growth and decay depends on the value of γ . If we would have added $i\gamma$ to the lower diagonal element of H_m^A , then the opposite would have happened, i.e., the state would have gone to $|1\rangle$.

Case B. We add $i\gamma$ to one of the diagonal elements but do not subtract it from the other diagonal. In a

sense, this is ‘‘pushing’’ the state towards one eigenvector without pulling it from the other. H_m^B looks like

$$H_m^B = \begin{bmatrix} \lambda_1 + i\gamma & 0 \\ 0 & \lambda_2 \end{bmatrix} = \left(\lambda_0 + \frac{i\gamma}{2} \right) \mathbb{I} + \left(\omega + \frac{i\gamma}{2} \right) \sigma_z.$$

So, $R_0 = \lambda_0 + \frac{i\gamma}{2}$, $R_3 = \omega + \frac{i\gamma}{2}$. In this case, $\rho^B(t)$ turns out to be

$$\rho^B(t) = \begin{bmatrix} \frac{|c_1|^2}{|c_1|^2 + |c_2|^2 e^{-2\gamma t}} & \frac{c_1 c_2^* e^{-i2\omega t}}{|c_1|^2 e^{\gamma t} + |c_2|^2 e^{-\gamma t}} \\ \frac{c_1^* c_2 e^{i2\omega t}}{|c_1|^2 e^{\gamma t} + |c_2|^2 e^{-\gamma t}} & \frac{|c_2|^2}{|c_1|^2 e^{2\gamma t} + |c_2|^2} \end{bmatrix} \quad (17)$$

which is exactly same as $\rho^A(t)$ except that γ is replaced by $\gamma/2$. So, the rate of convergence is halved.

Case C(i). Let us subtract $-i\gamma$ from the lower diagonal element. In this case

$$H_m^C = \begin{bmatrix} \lambda_1 & 0 \\ 0 & \lambda_2 - i\gamma \end{bmatrix} = \left(\lambda_0 - \frac{i\gamma}{2} \right) \mathbb{I} + \left(\omega + \frac{i\gamma}{2} \right) \sigma_z.$$

For this case, $\rho^{C_1}(t) = \rho^B(t)$ which means there is no difference in just pushing a state to an eigenvector or just pulling it away from the other.

Case C(ii). In this case, the Hamiltonian used is H_m^C but we would not use the trace normalisation in the evolution equation (2). So, $\rho^{C_2}(t) = N(t)$. The expression looks like

$$\rho^{C_2}(t) = \begin{bmatrix} |c_1|^2 & e^{-\gamma t} c_1 c_2^* e^{-i2\omega t} \\ e^{-\gamma t} c_1^* c_2 e^{i2\omega t} & |c_2|^2 e^{-2\gamma t} \end{bmatrix} \quad (18)$$

Here we see that all the terms go to 0 as $t \rightarrow \infty$ except $\rho_{11}^{C_2}(t)$ term which stays as it was initially. Therefore, if the density matrix represented an ensemble of particles, this evolution would leave the population in the ground state intact. There would be decay in the excited state population and also decoherence. If we would have subtracted $-i\gamma$ from the 1st element of $H_m(t)$, the only term remaining in the density matrix after evolution for a long time would be the excited state population.

The Lindblad master equation formalism [44–46] gives the evolution of a system state ρ_s which is in contact with the environment. As a result of the interaction with the environment, there is a loss of coherence such that given enough time, the density matrix state thermalizes to a mixed state with no off-diagonal terms. The diagonal terms sum up to one and each of those gives the population at different energy levels.

The C(ii) case leaves out a density matrix whose trace is not preserved, which means the particle number is not preserved. The ground state population remains as it is. But if we use a different Hamiltonian with $-i\gamma$ in the upper diagonal, we would be left with just the excited state population in the density matrix. Thus, the sum of these two dynamics has a unit trace and looks like the density matrix obtained from the Lindblad dynamics. The connection between master equation Lindblad-Kossakowski

type and non-Hermitian or pseudo-Hermitian dynamics has been studied before [47–49].

This means that the Lindblad Markovian dynamics can be obtained as an incoherent sum of two different non-Hermitian Hamiltonian dynamics.

V. CONCLUSION

We have given a dynamical model for collapse to a particular eigenstate of the Hamiltonian. We first showed that the evolution of a density matrix via a non-Hermitian Hamiltonian is dictated by a nonlinear von Neumann equation. Nonlinear analysis of this equation showed that a non-Hermitian Hamiltonian with complex eigenvalues will have an attractor eigenstate—one which has the largest imaginary part of the eigenvalue. Next, we designed the measurement Hamiltonian that has the chosen eigenstate as the stable fixed point. Then, we combined the two Hamiltonians—one operating outside the measurement interval and one inside—into one time-dependent Hamiltonian with a switching function. Being written in the eigenvector basis, this Hamiltonian is also diagonal. We also showed that this formalism can be extended easily to N -dimensional Hilbert space and that the largest imaginary part of the eigenvalues must be unique for collapse to happen. Finally, we considered three non-

Hermitian Hamiltonians and calculated the expressions of time-evolved density matrices in each case. In one of the cases, it was seen that the Lindblad-type evolution in open quantum systems can be obtained as an incoherent sum of two different non-Hermitian Hamiltonian dynamics.

Our model shows what happens in the system subspace when a collapse happens. One can use a Naimark dilation protocol [50] to dilate our non-Hermitian Hamiltonian to a higher dimensional Hermitian Hamiltonian that governs the system-ancilla state. The embedding of a non-Hermitian \mathcal{PT} -symmetric Hamiltonian into a higher dimensional Hermitian one has already been studied previously [43, 51–55]. Applying this protocol in our model will give us an interaction Hamiltonian that accounts for unitary evolution of the system-ancilla state while the system subspace undergoes non-Hermitian dynamics exactly as shown in this paper. This is under investigation and will be reported elsewhere.

ACKNOWLEDGEMENT

We would like to thank Sourin Das, Rangeet Bhatlacharyya, Anant Varma, and Arnab Acharya for useful discussions. S.B. acknowledges the J.C. Bose National Fellowship provided by SERB, Government of India, Grant No. JBR/2020/000049.

-
- [1] J. J. Sakurai and J. Napolitano, *Modern Quantum Mechanics*, 2nd ed. (Cambridge University Press, 2017).
- [2] M. A. Nielsen and I. L. Chuang, *Quantum Computation and Quantum Information* (Cambridge University Press, 2010).
- [3] P. Marage and G. Wallenborn, The debate between Einstein and Bohr, or how to interpret quantum mechanics, in *The Solway Councils and the Birth of Modern Physics*, edited by P. Marage and G. Wallenborn (Birkhäuser Basel, Basel, 1999) pp. 161–174.
- [4] A. Einstein, B. Podolsky, and N. Rosen, Can quantum-mechanical description of physical reality be considered complete?, *Phys. Rev.* **47**, 777 (1935).
- [5] J. Faye, *The Stanford Encyclopedia of Philosophy*, Winter 2019 ed., edited by E. N. Zalta (Metaphysics Research Lab, Stanford University, 2019).
- [6] D. Bohm, A suggested interpretation of the quantum theory in terms of “hidden” variables. i, *Phys. Rev.* **85**, 166 (1952).
- [7] H. Everett, “relative state” formulation of quantum mechanics, *Rev. Mod. Phys.* **29**, 454 (1957).
- [8] E. Wigner, Remarks on the mind-body problem, *The scientist speculates*, 284 (1961).
- [9] G. C. Ghirardi, A. Rimini, and T. Weber, Unified dynamics for microscopic and macroscopic systems, *Phys. Rev. D* **34**, 470 (1986).
- [10] P. Pearle, Combining stochastic dynamical state-vector reduction with spontaneous localization, *Phys. Rev. A* **39**, 2277 (1989).
- [11] G. C. Ghirardi, P. Pearle, and A. Rimini, Markov processes in hilbert space and continuous spontaneous localization of systems of identical particles, *Phys. Rev. A* **42**, 78 (1990).
- [12] L. Diósi, Models for universal reduction of macroscopic quantum fluctuations, *Phys. Rev. A* **40**, 1165 (1989).
- [13] R. Penrose, On gravity’s role in quantum state reduction, *General Relativity and Gravitation* **28**, 581 (1996).
- [14] C. Rovelli, Relational quantum mechanics, *International Journal of Theoretical Physics* **35**, 1637 (1996).
- [15] W. H. Zurek, Decoherence, einselection, and the quantum origins of the classical, *Rev. Mod. Phys.* **75**, 715 (2003).
- [16] J. S. Bell, On the Einstein Podolsky Rosen paradox, *Physics Physique Fizika* **1**, 195 (1964).
- [17] C. H. Bennett, G. Brassard, C. Crépeau, R. Jozsa, A. Peres, and W. K. Wootters, Teleporting an unknown quantum state via dual classical and Einstein-Podolsky-Rosen channels, *Phys. Rev. Lett.* **70**, 1895 (1993).
- [18] A. Aspect, Bell’s inequality test: more ideal than ever, *Nature* **398**, 189 (1999).
- [19] J. Åke Larsson, Loopholes in Bell inequality tests of local realism, *Journal of Physics A: Mathematical and Theoretical* **47**, 424003 (2014).
- [20] A. J. Leggett and A. Garg, Quantum mechanics versus macroscopic realism: Is the flux there when nobody looks?, *Phys. Rev. Lett.* **54**, 857 (1985).
- [21] J. F. Clauser, M. A. Horne, A. Shimony, and R. A. Holt, Proposed experiment to test local hidden-variable theories, *Phys. Rev. Lett.* **23**, 880 (1969).
- [22] C. M. Bender and S. Boettcher, Real spectra in non-

- Hermitian Hamiltonians having \mathcal{PT} -symmetry, *Phys. Rev. Lett.* **80**, 5243 (1998).
- [23] C. M. Bender, S. Boettcher, and P. N. Meisinger, \mathcal{PT} -symmetric quantum mechanics, *Journal of Mathematical Physics* **40**, 2201 (1999), <https://doi.org/10.1063/1.532860>.
- [24] P. D. Mannheim, Antilinearity rather than Hermiticity as a guiding principle for quantum theory, *Journal of Physics A: Mathematical and Theoretical* **51**, 315302 (2018).
- [25] R. El-Ganainy, K. G. Makris, M. Khajavikhan, Z. H. Musslimani, S. Rotter, and D. N. Christodoulides, Non-hermitian physics and \mathcal{PT} -symmetry, *Nature Physics* **14**, 11 (2018).
- [26] Y. Ashida, Z. Gong, and M. Ueda, Non-hermitian physics, *Advances in Physics* **69**, 249 (2020).
- [27] A. Guo, G. J. Salamo, D. Duchesne, R. Morandotti, M. Volatier-Ravat, V. Aimez, G. A. Siviloglou, and D. N. Christodoulides, Observation of \mathcal{PT} -symmetry breaking in complex optical potentials, *Phys. Rev. Lett.* **103**, 093902 (2009).
- [28] S. Longhi, Bloch oscillations in complex crystals with \mathcal{PT} -symmetry, *Phys. Rev. Lett.* **103**, 123601 (2009).
- [29] C. E. Rüter, K. G. Makris, R. El-Ganainy, D. N. Christodoulides, M. Segev, and D. Kip, Observation of parity-time symmetry in optics, *Nature Physics* **6**, 192 (2010).
- [30] C. Bender, B. Berntson, D. Parker, and E. Samuel, Observation of \mathcal{PT} phase transition in a simple mechanical system, *American Journal of Physics* **81** (2012).
- [31] N. Bender, S. Factor, J. D. Bodyfelt, H. Ramezani, D. N. Christodoulides, F. M. Ellis, and T. Kottos, Observation of asymmetric transport in structures with active nonlinearities, *Phys. Rev. Lett.* **110**, 234101 (2013).
- [32] T. Wang, J. Fang, Z. Xie, N. Dong, Y. N. Joglekar, Z. Wang, J. Li, and L. Luo, Observation of two \mathcal{PT} transitions in an electric circuit with balanced gain and loss, *The European Physical Journal D* **74**, 167 (2020).
- [33] J. Schindler, A. Li, M. C. Zheng, F. M. Ellis, and T. Kottos, Experimental study of active LRC circuits with \mathcal{PT} symmetries, *Phys. Rev. A* **84**, 040101 (2011).
- [34] S. Bittner, B. Dietz, U. Günther, H. L. Harney, M. Miski-Oglu, A. Richter, and F. Schäfer, \mathcal{PT} symmetry and spontaneous symmetry breaking in a microwave billiard, *Phys. Rev. Lett.* **108**, 024101 (2012).
- [35] V. V. Konotop, J. Yang, and D. A. Zezyulin, Nonlinear waves in \mathcal{PT} -symmetric systems, *Rev. Mod. Phys.* **88**, 035002 (2016).
- [36] J.-S. Tang, Y.-T. Wang, S. Yu, D.-Y. He, J.-S. Xu, B.-H. Liu, G. Chen, Y.-N. Sun, K. Sun, Y.-J. Han, C.-F. Li, and G.-C. Guo, Experimental investigation of the no-signalling principle in parity-time symmetric theory using an open quantum system, *Nature Photonics* **10**, 642 (2016).
- [37] J. Li, A. K. Harter, J. Liu, L. de Melo, Y. N. Joglekar, and L. Luo, Observation of parity-time symmetry breaking transitions in a dissipative Floquet system of ultracold atoms, *Nature Communications* **10**, 855 (2019).
- [38] F. Klauck, L. Teuber, M. Ornigotti, M. Heinrich, S. Scheel, and A. Szameit, Observation of \mathcal{PT} -symmetric quantum interference, *Nature Photonics* **13**, 883 (2019).
- [39] P. D. Mannheim, Appropriate inner product for \mathcal{PT} -symmetric Hamiltonians, *Phys. Rev. D* **97**, 045001 (2018).
- [40] D. C. Brody and E.-M. Graefe, Mixed-state evolution in the presence of gain and loss, *Phys. Rev. Lett.* **109**, 230405 (2012).
- [41] N. Gisin, A simple nonlinear dissipative quantum evolution equation, *Journal of Physics A: Mathematical and General* **14**, 2259 (1981).
- [42] P. D. Mannheim, Appropriate inner product for \mathcal{PT} -symmetric Hamiltonians, *Phys. Rev. D* **97**, 045001 (2018).
- [43] Y. Wu, W. Liu, J. Geng, X. Song, X. Ye, C.-K. Duan, X. Rong, and J. Du, Observation of parity-time symmetry breaking in a single-spin system, *Science* **364**, 878 (2019).
- [44] R. Ingarden and A. Kossakowski, On the connection of nonequilibrium information thermodynamics with non-hamiltonian quantum mechanics of open systems, *Annals of Physics* **89**, 451 (1975).
- [45] V. Gorini, A. Kossakowski, and E. C. G. Sudarshan, Completely positive dynamical semigroups of n-level systems, *Journal of Mathematical Physics* **17**, 821 (1976).
- [46] G. Lindblad, On the generators of quantum dynamical semigroups, *Communications in Mathematical Physics* **48**, 119 (1976).
- [47] K. G. Zloshchastiev and A. Sergi, Comparison and unification of non-Hermitian and Lindblad approaches with applications to open quantum optical systems, *Journal of Modern Optics* **61**, 1298 (2014).
- [48] G. Sclarici and L. Solombrino, Time evolution of non-Hermitian quantum systems and generalized master equations, *Czechoslovak Journal of Physics* **56**, 935 (2006).
- [49] A. S. Matsoukas-Roubeas, F. Roccati, J. Cornelius, Z. Xu, A. Chenu, and A. del Campo, Non-hermitian hamiltonian deformations in quantum mechanics, *Journal of High Energy Physics* **2023**, 60 (2023).
- [50] A. Holevo, *Probabilistic and Statistical Aspects of Quantum Theory*, Publications of the Scuola Normale Superiore (Scuola Normale Superiore, 2011).
- [51] U. Günther and B. F. Samsonov, Naimark-dilated \mathcal{PT} -symmetric brachistochrone, *Phys. Rev. Lett.* **101**, 230404 (2008).
- [52] K. Kawabata, Y. Ashida, and M. Ueda, Information retrieval and criticality in parity-time-symmetric systems, *Phys. Rev. Lett.* **119**, 190401 (2017).
- [53] M. Huang, A. Kumar, and J. Wu, Embedding, simulation and consistency of \mathcal{PT} -symmetric quantum theory, *Physics Letters A* **382**, 2578 (2018).
- [54] M. Huang, R.-K. Lee, L. Zhang, S.-M. Fei, and J. Wu, Simulating broken \mathcal{PT} -symmetric hamiltonian systems by weak measurement, *Phys. Rev. Lett.* **123**, 080404 (2019).
- [55] A. V. Varma and S. Das, Simulating many-body non-Hermitian \mathcal{PT} -symmetric spin dynamics, *Phys. Rev. B* **104**, 035153 (2021).